A COMPARISON OF METHODS FOR MEASUREMENT OF PRESSURE IN HYDRAULIC LINES

Susan Sprague and Andrew Chorney
Naval Air Warfare Center Aircraft Division

ABSTRACT

This presentation summarizes a study characterizing strain gages and pressure transducers used to measure the fluid pressure within aircraft hydraulic lines. A series of laboratory calibrations and finite element analyses was performed to demonstrate the quality of data from both pressure transducers and strain gages under variations in both temperature and external strains on the hydraulic lines. Strain gages showed a marked susceptibility to external strains on hydraulic lines, and wide variations in susceptibility to temperature changes. Pressure transducers were found to be relatively immune to both conditions. It is recommended that strain gages be used for trend data only.

KEY WORDS

Strain gages, pressure transducers, hydraulic lines, measurement uncertainty, and aircraft.

INTRODUCTION

Measurement of a parameter can often be achieved using a variety of methods. The choice of methodology is made according to the requirements of the application. Considerations include the type of measurement; transducer specificity; electrical, physical, and mechanical characteristics; data requirements; and program constraints. In most cases the choice of transducer involves a trade-off. For example, the most accurate transducer may be too large, too heavy, or too expensive to be suitable for the application.

In 1996 an aircraft at NAWCAD was instrumented for measurement of fluid pressure within several hydraulic lines. Two methodologies were used to measure the pressure: externally placed strain gages to measure the hoop stress on the lines exerted by the hydraulic fluid within the lines (indirect pressure measurement), and pressure transducers inserted within the lines to measure the pressure of the hydraulic fluid (direct pressure measurement)

The choice of methodology was based on trade-off considerations:

- Type of measurement: fluid pressure. Transducers measure the pressure directly. Strain gages measure minute changes in the outside diameter of the lines, from which the pressure within is inferred.
- Specificity: Transducers are highly specific to pressure, with minimal cross-reaction to other physical influences. Strain gages are highly specific to expansion, contraction, or other movement of the outside surface. Special considerations are required to limit the cross-reaction of the strain gages to hoop stresses in the lines that are not caused by pressure from within. The strain gages were installed in such a manner that forces acting in opposing directions on opposite sides of the line (such as bending forces) would be cancelled out.
- Electrical: The output of the strain gages used was 0 to 10 millivolts, necessitating high signal conditioning gains. Pressure transducers output 0 to 200 millivolts, thus requiring lower signal conditioning gains and less susceptibility to noise and signal conditioning errors. In other respects, both transducer types are electrically suitable for the application.
- Physical: Transducers require insertion into the lines. The local configuration of the lines must be altered. Additionally, these transducers, though small, add measurable weight at the point of insertion, and measurable volume to the overall hydraulic system. Care must be taken to insure that these alterations do not affect the pressure under test or the integrity of the hydraulic lines and of the overall hydraulic system. Strain gages require no reconfiguration of the lines, and add negligible weight.
- Mechanical: Transducers require an invasive modification to the test article, and therefore safety of flight may be adversely impacted. They are, however, relatively easy to replace (maintainability) in the event of a failure – approximately one day turn-around. Strain gages require almost no modification to the test article, and therefore the impact to safety of flight is minimal. However, they require several days or weeks to replace in the event of a failure. Both transducer types were judged to be equally reliable under the full flight environment.
- Data: Transducers were expected to be superior to the strain gages in terms of measurement accuracy. The extent of this superiority was in question at the time of the installation. The frequency response of both transducer types was judged to be suitable for the application.
- Program constraints: The program was able to accept the cost and schedule impacts of either type of transducer.

The highest priority in the considerations above was given to safety of flight, with data accuracy the second priority. Therefore the strain gages were determined to be the method of choice for flight testing whenever possible. Since the accuracy of the gages was in question, a series of ground tests was conducted using both transducer types simultaneously for comparison of results. In all cases the transducer data was considered to be “truth data” and the strain gage data was evaluated against the truth data. The ground test results were included in the final decision process concerning which transducer type to use during flight-testing. The final configuration was a combination of transducers and strain gages that best met the requirements of the program. During the ensuing series of test flights anomalies were noted in the strain gage data including an unusual drifting characteristic. In some cases this drifting characteristic was severe enough to preclude reliable interpretation of the results.

In order to better characterize the drift characteristics and overall accuracy of the strain gages a series of post-flight-test calibrations was undertaken under varying conditions of temperature and strain on the lines.

METHODOLOGY

Since the cost and time available to perform the post calibrations was not infinite, the project engineer was consulted for determination of which lines to test. One each of the "best" and "worst" lines was chosen for characterization. The characterizations were performed on LEF2LSO (best) and LEF5LHDU (worst). Each line was subjected to calibration under a variety of combinations of temperature and strain, with the output from a transducer and the existing strain gages being measured simultaneously. Additionally, the lines were modeled using finite element analysis (FEA). The results of the calibrations were analyzed for measurement uncertainty, and used for verification of the FEA models. Once the FEA models were validated further strains were applied to the models in order to obtain additional characterization data.

Experimental setup: The experimental set-up was designed to test the response of both transducer types to temperature changes, and to test the response of the strain gages to strains on the hydraulic lines that were not due to internal pressure. Strains on the hydraulic lines were not expected to affect the conventional pressure transducers, so less emphasis was placed on subjecting these to external strains. However, when it was feasible to do so, the conventional pressure transducers were subjected to the same strains as were the strain gages.

Analysis of Measurement Uncertainty: The Abernethy Measurement Uncertainty Method was used for the uncertainty analysis. Systematic (bias) error and random (scatter) error were determined separately, then combined for an overall estimate of the 95% uncertainty ranges. In this paper the terms bias and scatter will be used instead of systematic and random error in order to reduce confusion with the symbols b and s used in the applicable equations. The calculations and numeric results may be found in Appendix A.

Conditions: Calibrations were run at various temperatures and strain conditions. Transducer outputs were measured at pressures of 0, 500, 1000, 1500, and 2000 psig (pounds per square inch, gage). Calibration runs were performed at temperatures of 32°F, 70°F, 100°F, 150°F, and 200°F, and under strain conditions of no strain (Un), compression (C), tension (T), and bending in two directions (Up and D).

Data Manipulation: The error sources for each post-calibration run were temperature and strain. The results of the calibrations performed on unstrained lines at 70°F (nominal room temperature) at each pressure level were used as the "truth" values for those pressure levels. All results were converted to % of full scale so that the two methodologies (pressure transducer and strain gage) could be directly compared. See Appendix A for details.

Finite Element Analysis: The decision to use FEA was not made until after the first series of calibrations had been run, including the compression runs on the "good" line. As a consequence of this late decision, the compression runs on this line were performed at an unknown level of compression.

Unfortunately, that series of runs presented an anomaly that could not be explained: the experimental results could not be duplicated using the FEA model.

RESULTS

The results of this study indicated that the measurement of hydraulic pressure using external strain gages is considerably less accurate than when pressure transducers are used. The strain gages are highly subject to cross-reactions due to movement and stresses on the hydraulic lines. Temperature compensation on the strain gages was very good in one case (LEF2LSO), and very poor in the other (LEF5LHDU).

Overall parameter measurement uncertainty: The overall values are shown in Table 1 below. The abbreviation "XDCR" is used to indicate a pressure transducer.

Table 1: Overall measurement uncertainty

Parameter	Transducer	B	S	U95
LEF2LSO	Strain Gage	0.53%	9.18%	18.37%
LEF2LSO	XDCR	0.27%	1.28%	2.57%
LEF5LHDU	Strain Gage	-4.05%	11.00%	22.37%
LEF5LHDU	XDCR	0.04%	1.06%	2.11%

Most of the strain gage error was displayed as offset of the y-intercept, with very little error due to slope changes (see Appendix A and graphs below). Each individual run showed relatively little scatter. The width of the peaks in the %Error graphs is therefore directly related to error input from the opposing source (Force or Temperature). The primary error source for the LEF2LSO strain gage was found to be external strain. The LEF5LHDU strain gage responded to changes in both external strain and temperature. It is reasonable to expect that bias error would be introduced when the lines were installed in the aircraft. Bias error due to external strain induced at installation of the line can be zeroed out through signal conditioning. Under flight conditions drifting anomalies as the lines undergo strains caused by structural shifts, heating, vibration, and g-forces along three axes can be expected. This error can not be zeroed out through signal conditioning.

Most of the pressure transducer error was produced at high temperature (150°F and 200°F). The specifications on these transducers stated that they were compensated to 180°F, so these results were not surprising. However, the overall uncertainty was less than 2.6% – far superior to the 18% to 22% uncertainties seen with the strain gages. The LEF5LHDU transducer also displayed a relatively high offset during a single run – compression at 200°. Therefore, both the compression data and the 200° data for that transducer showed relatively high uncertainties (3.41% and 4.17% respectively).

The data is illustrated below in two forms: % Error graphs, and corresponding point pair graphs. The % Error graphs were generated as follows: the normal distribution for each grouping was calculated in MS Excel from the bias (average) and scatter (standard deviation) values, and the resulting bell curves were added together point-wise along the x-axis. The normal distribution curve for the overall (ungrouped) data is multiplied by 5 and superimposed for comparison. The overall (ungrouped) U_{95} values are indicated as vertical lines. The peaks in the % Error graphs correspond from left to right to the lines in

the Point Pair graphs from bottom to top. The calculations and numerical data used to generate these graphs may be found in Appendix A.

Figure 1: LEF2LSO Strain Gage Data by Force Type, % Error and Point Pair Graphs

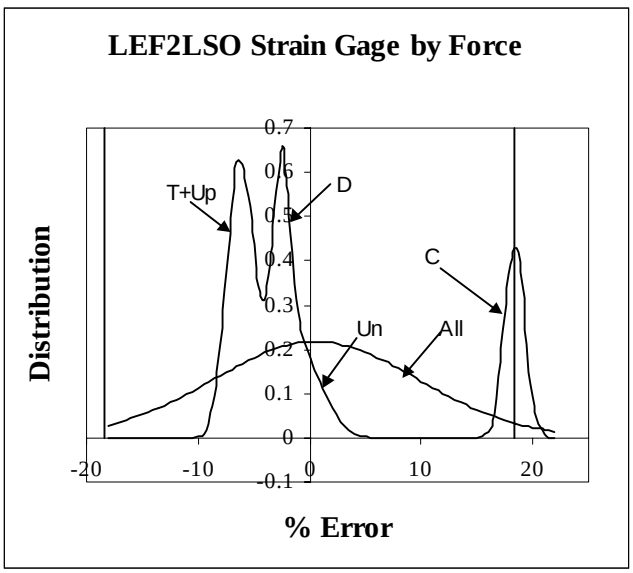

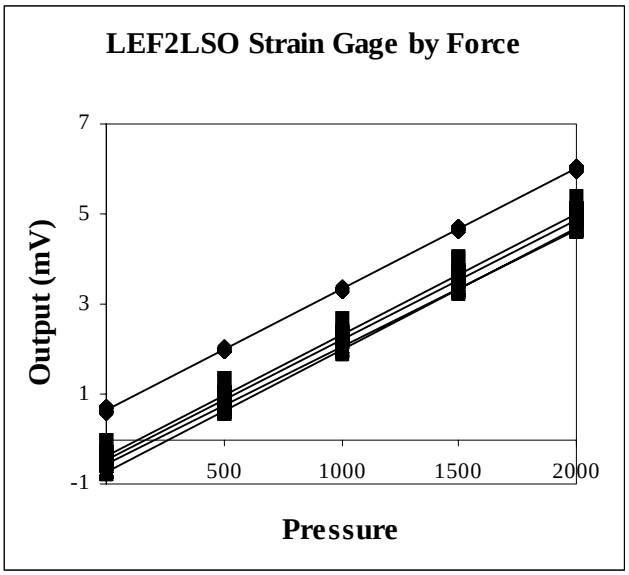

Figure 2: LEF2LSO Pressure Transducer Data by Force Type, %Error and Point Pair Graphs

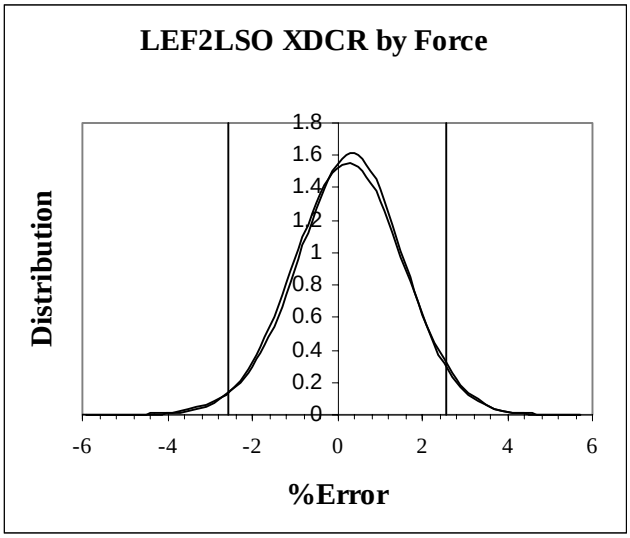

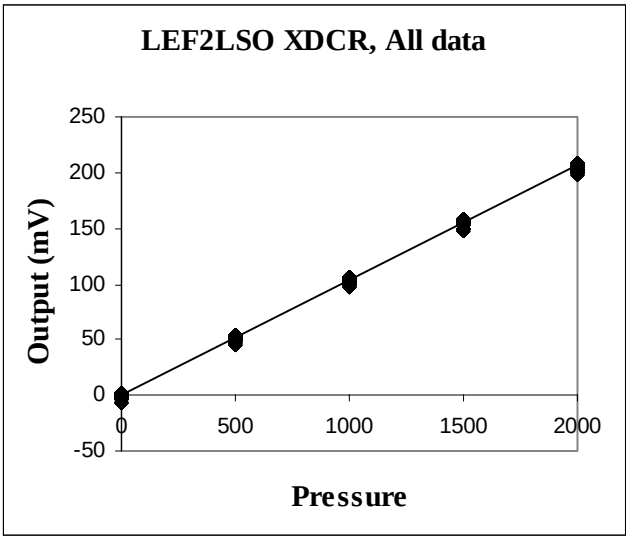

Force Effects: Force effects are analyzed over all temperatures together. It should be noted that LEF2LSO is fully characterized, while LEF5LHDU is only partially characterized due to time and budget constraints. Post calibrations were performed on LEF2LSO at all combinations of temperature and force type. Post calibrations were performed on LEF5LHDU at all temperatures only in the unstrained state. Force runs were conducted only at 70° and 200°.

LEF2LSO: The effect of external forces on the strain gage data is dramatic and obvious. It can be seen that the scatter data (seen as the bell-curve spread) is considerably lower under any one force type than when all data points (ungrouped) are considered together.

The pressure transducer, as expected, was relatively immune to external forces on the hydraulic line. For the transducer data no attempt was made to group point pair data by force type. Instead all data was plotted and a single LSBF line was calculated for all data points. The reason is that the scatter is so low as to put all force types virtually on top of each other.

Figure 3:LEF5LHDU Strain Gage Data by Force Type, %Error and Point Pair Graphs

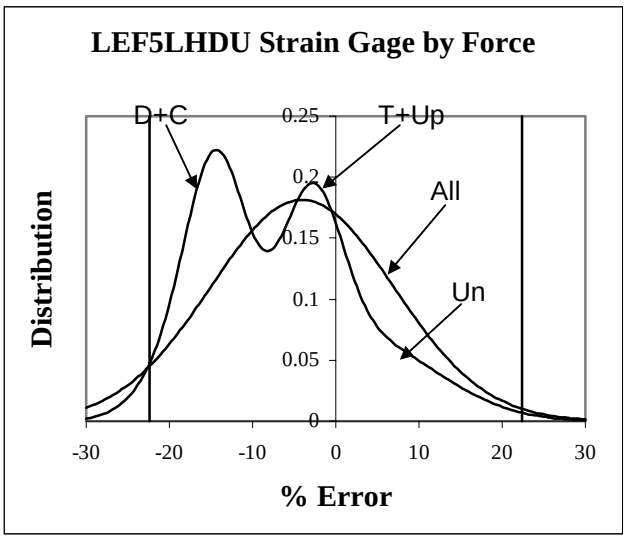

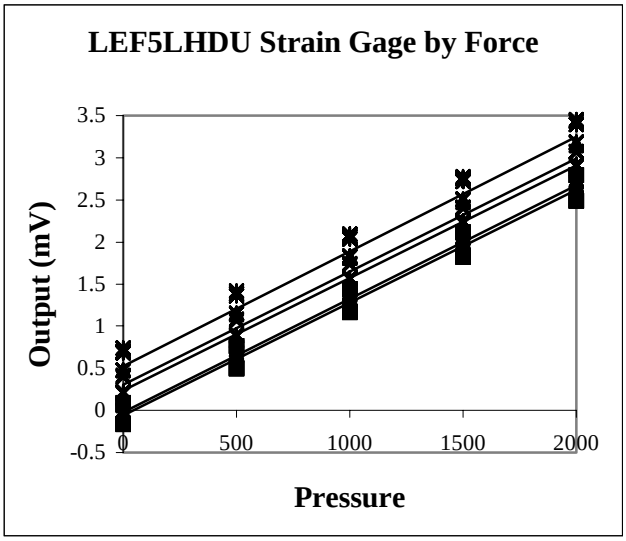

Figure 4: LEF5LHDU Pressure Transducer Data by Force Type, %Error and Point Pair Graphs

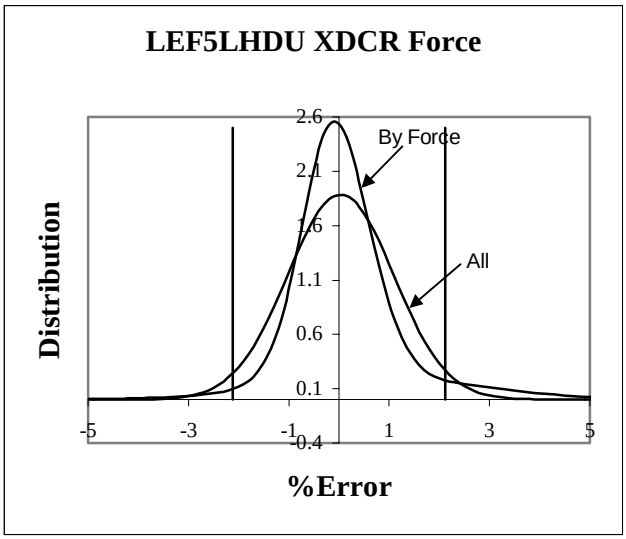

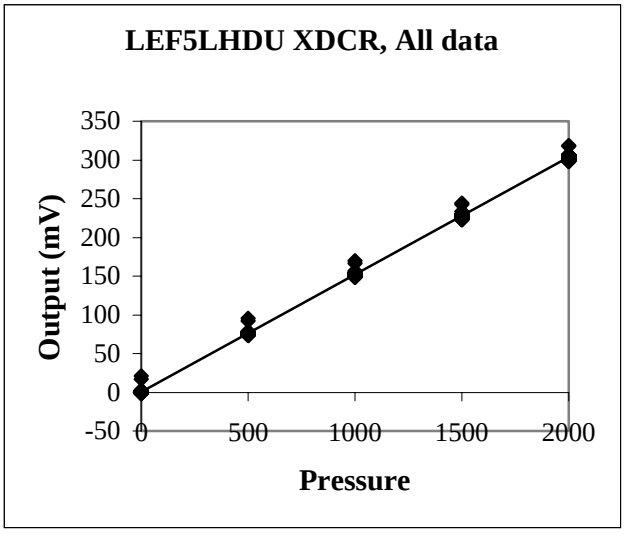

LEF5LHDU: The effect of external forces on the strain gage data is again dramatic and obvious. This time, though, there was less separation of the peaks. The probable reason will be seen in the temperature analysis.

The pressure transducer, as expected, was relatively immune to external forces on the hydraulic line. Note on the apparent scatter for the LEF5LHDU pressure transducer: the points above the LSBF line are due to a single point-pair run (up and back down) out of a total of 44. The other 43 fall on the LSBF line and are the reason that the graph "looks" worse than the calculated scatter and correlation.

Temperature Effects: Temperature effects are analyzed over all forces together. As was noted above, LEF2LSO is fully characterized, while LEF5LHDU is only partially characterized due to time and budget constraints. Post calibrations were performed on LEF2LSO at all combinations of temperature and force type. Post calibrations were performed on LEF5LHDU at all temperatures only in the unstrained state. Force runs were conducted only at 70° and 200°. The temperature effects on the unstrained runs for both parameters are shown at the end of the graphs below for comparison. Note that the 200° error was part of the rightmost peak in the unstrained LEF5LHDU case, but "migrated" to the overall error in the Temperature %Error plot. That was the only temperature (other than 70°) that was used for all force types. It is possible but unlikely that the 32°, 100°and 150° offsets seen in the unstrained temperature would also have merged into the overall data if they had been run at all force types. It is unlikely because no such distinct temperature peaks were observed in the LEF2LSO (perfectly temperature compensated) case, even with unstrained data alone.

Figure 5: LEF2LSO Strain Gage Data by Temperature, % Error and Point Pair Graphs

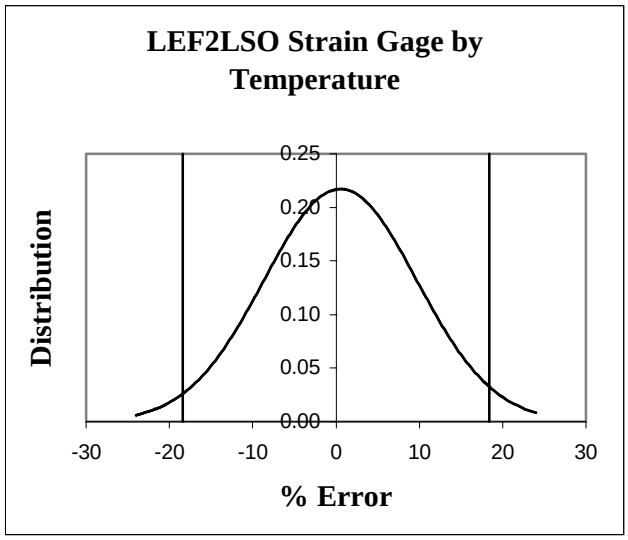

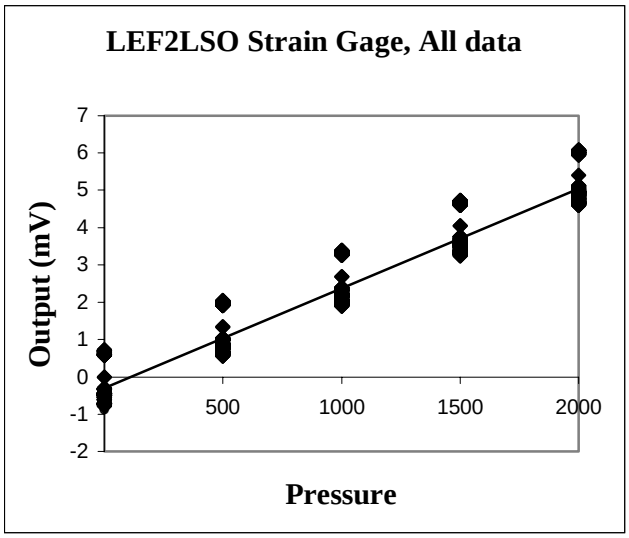

LEF2LSO: Upon examination of the temperature effects it can be seen that for the LEF2LSO strain gage the data at all temperatures is nearly identical to the overall data. The interpretation is that the temperature compensation for this strain gage is nearly perfect, and the relatively high scatter is due solely to force effects.

Figure 6: LEF2LSO Pressure Transducer Data by Temperature, % Error and Point Pair Graphs

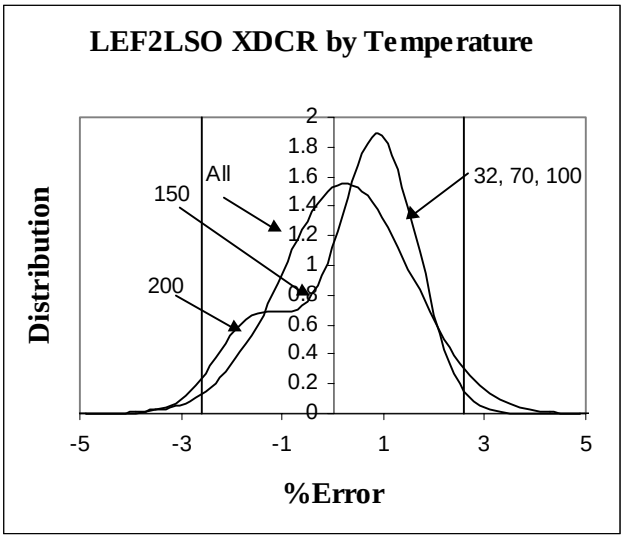

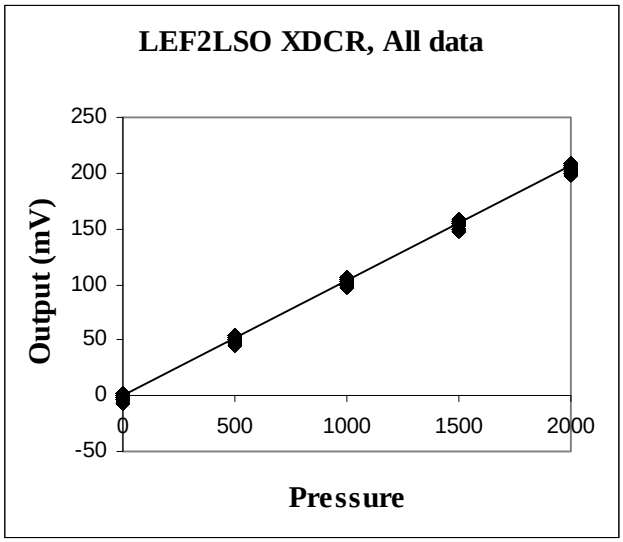

The pressure transducer showed error responses to higher temperatures. This was not surprising, since this transducer was temperature compensated only to 180°. The overall error for this transducer even at 200° was less than 3%.

Figure 7: LEF5LHDU Strain Gage Data by Temperature, % Error and Point Pair Graphs

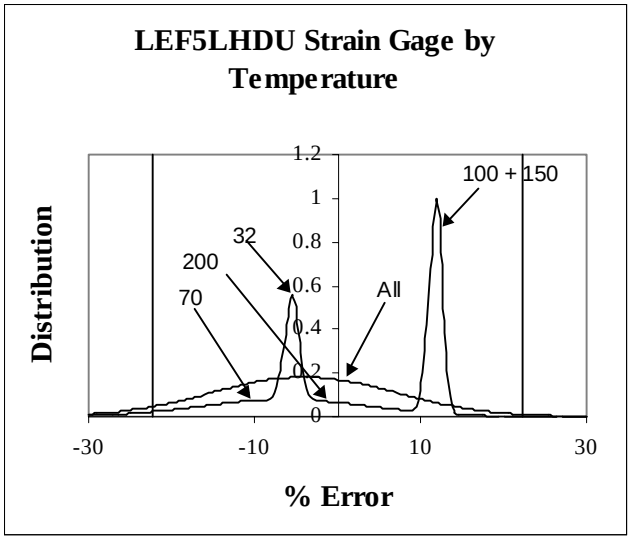

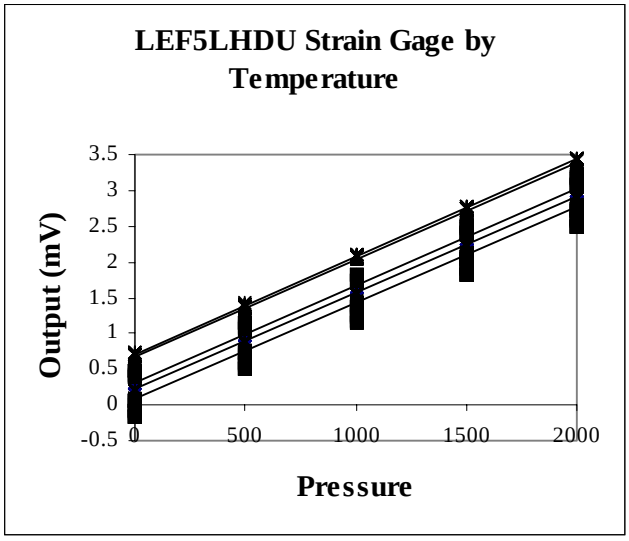

LEF5LHDU: The LEF5LHDU strain gage shows poor temperature compensation. It is possible, though, that the results would be different had all forces been run at all temperatures. The temperature

data for the unstrained strain gages (both LEF2LSO and LEF5LHDU) is shown below for comparison. It may be noted that the 200° peak in the LEF5LHDU plot below has migrated to the underlying spread in the plot above. It is possible that the other temperature peaks would have done the same. On the other hand, the LEF2LSO unstrained data showed very good temperature compensation even in the unstrained case. The interpretation of the LEF5LHDU temperature data remains ambiguous.

Figure 8: Unstrained Temperature Data for Both Strain Gages (LEF2LSO and LEF5LHDU), % Error Graphs

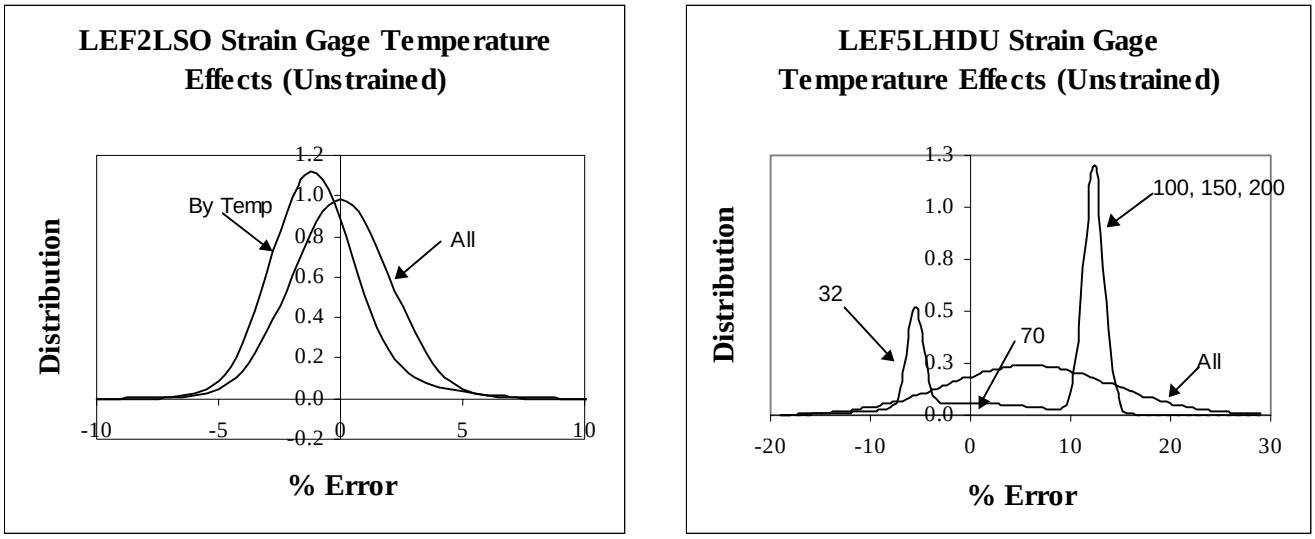

Figure 9: LEF5LHDU Pressure Transducer Data by Temperature, % Error and Point Pair Graphs

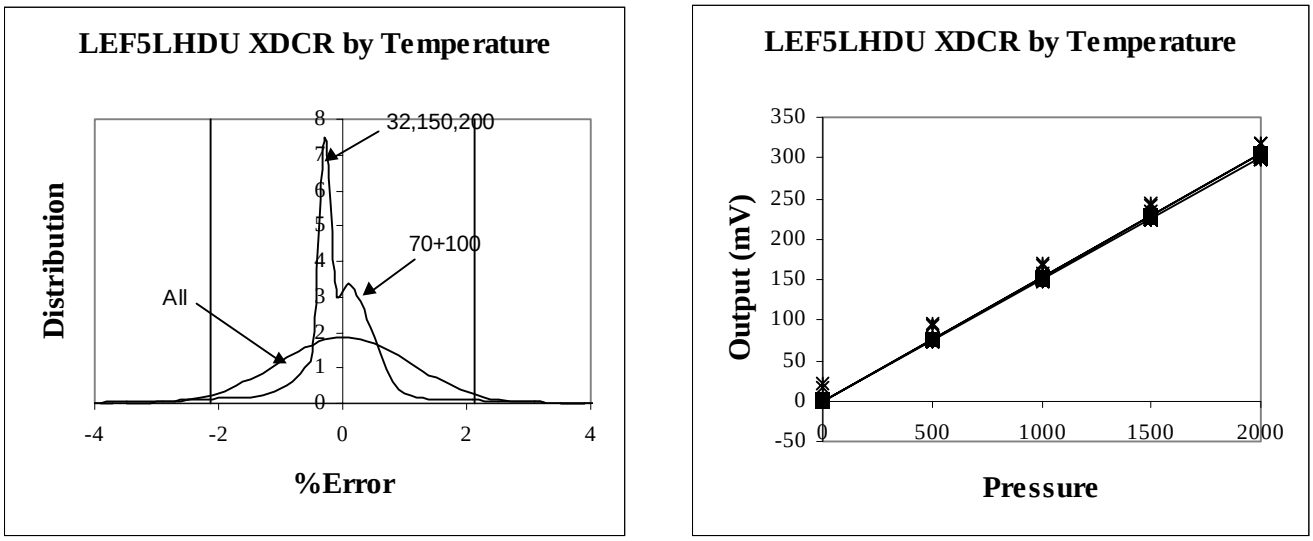

The pressure transducers displayed two distinct peaks, but neither peak was centered at more than 1% error, and both peaks showed very low scatter.

FINITE ELEMENT CORRELATION

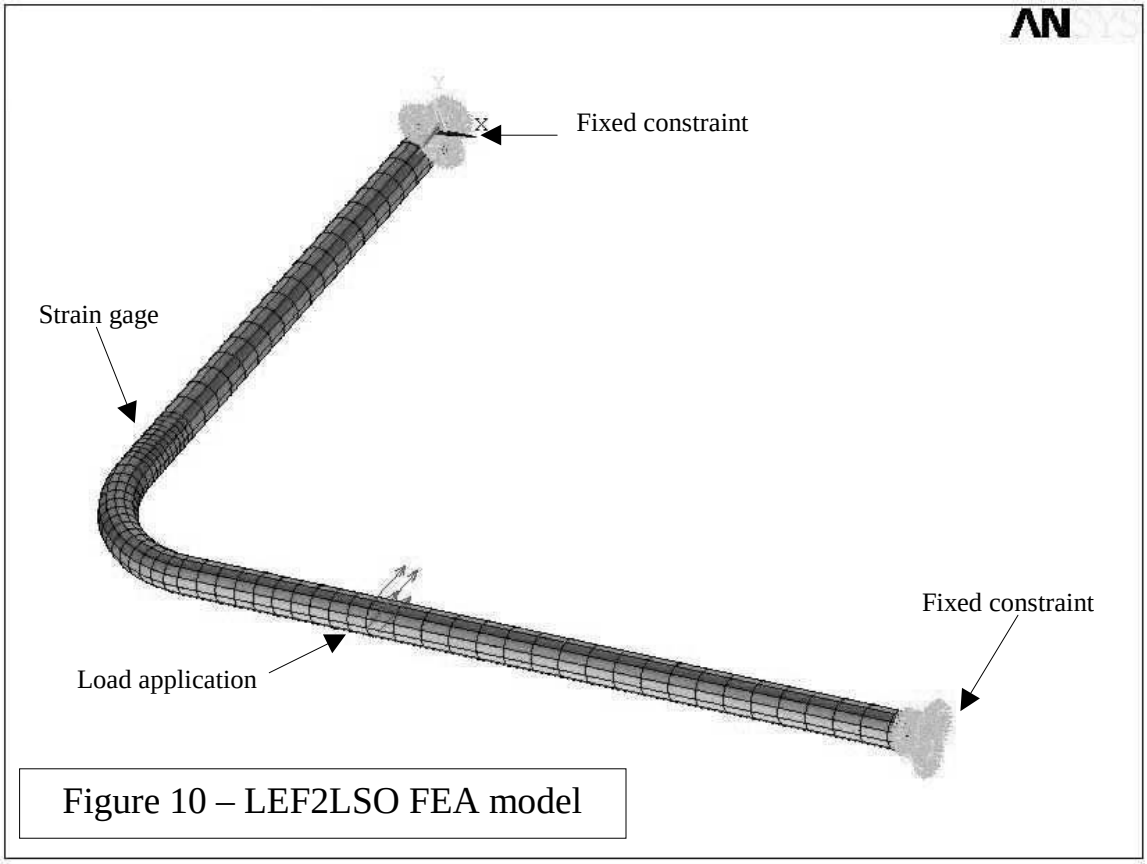

Figure 10 – LEF2LSO FEA model

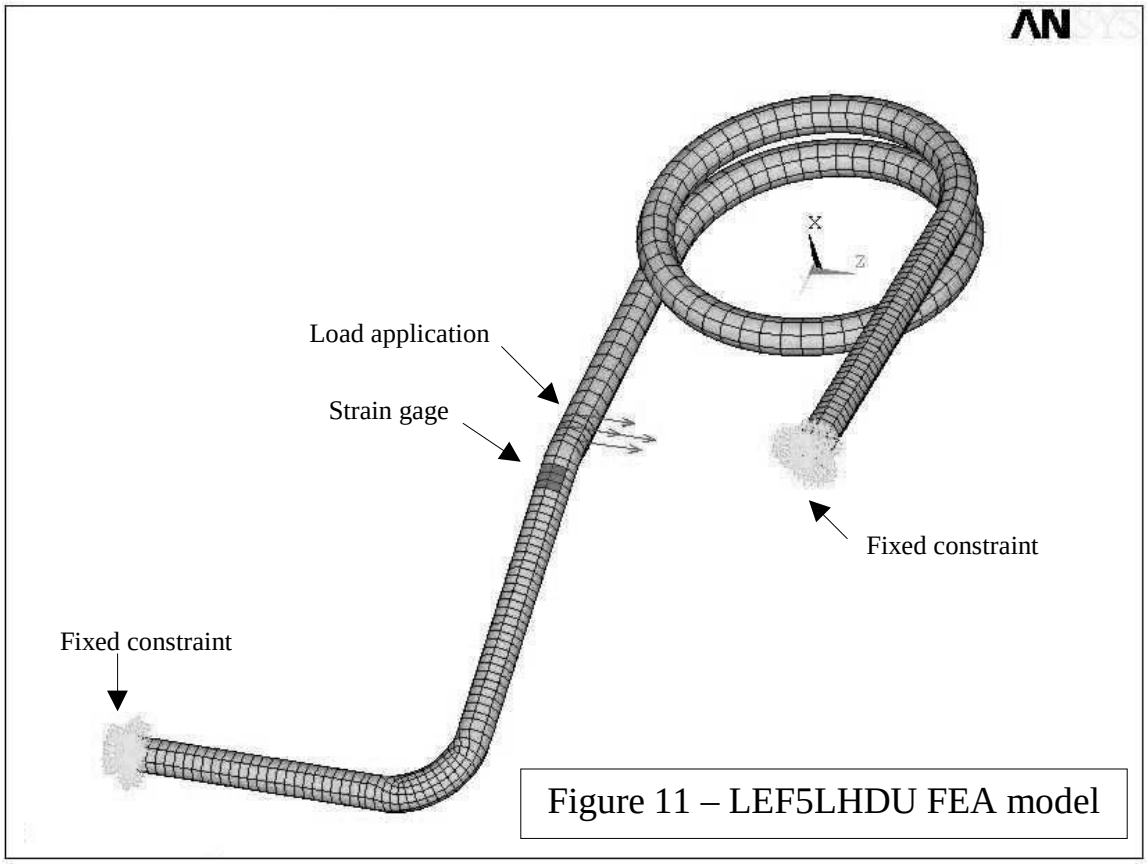

Figure 11 – LEF5LHDU FEA model

FEA models were built for the LEF2LSO (Figure 10) and LEF5LHDU (Figure 11) hydraulic lines. One of the purposes of FEA was to provide a separate benchmark from which to evaluate the experimental results of the strain gage calibrations. However, it was also hoped that once results from FEA were validated with respect to the experimental results and theoretical calculations, new test conditions that were not undertaken with the actual lines could be "virtually" tested through FEA.

FEA information: Pro/E Version 20 was used to construct the CAD models of the hydraulic lines. These models were then exported to ANSYS 5.5 via IGES files in order to conduct the FEA. Shell elements (SHELL93 and SHELL63) were used to model the geometry, although solid elements (SOLID45) and pipe elements (PIPE16 and PIPE18) were also evaluated. The slight gain in accuracy achieved with solid elements was coupled with a large increase in analysis run time. Pipe elements allowed hoop stress to be more directly measured and had quick run times, but they did not allow any static loads to be applied. Shell elements provided the most flexibility along with reasonable run times, so they were utilized. As noted in figures 11 and 12, fixed constraints were imposed at the ends of both lines. Elements at the strain gage locations were isolated in order to read hoop stresses at that location.

Loading conditions: Internal pressure loads identical to those carried out in the experimental calibrations were imposed on the FEA model, yielding load cases of 500, 1000, 1500, and 2000 psi. Runs with temperature differences were conducted on the LEF2LSO model, yielding four more load cases at 0, 32, 150, and 200 degrees Fahrenheit. However, the difference in hoop stress due to temperature was negligible, so FEA temperature runs were not conducted for LEF5LHDU. This is as expected, as the lines should primarily respond to temperature in the axial, not radial direction. Hoop stress is measured tangent to the outside diameter of the line due to radial expansion or contraction, so there should only be minute changes in hoop stress due to temperature. In addition, since the strain gages were to be temperature-compensated, in theory there should be no change in hoop stress (although as mentioned the temperature compensation on the LEF5LHDU line is questionable). As in the experimental calibrations, four different static loads were applied to each line, although as noted the compressive load on LEF2LSO is unknown as load cells were not part of the experimental setup until after that calibration was completed. Combinations of pressure and static load cases were combined to yield FEA data that could be compared to the experimental data. In addition, torque loads in the clockwise (CW) and counter-clockwise (CCW) directions were applied to the LEF2LSO model to evaluate their effect. The resulting hoop stress change was negligible in the CW direction but a significant increase in stress was observed in the CCW application of torque. Data from the FEA runs can be found in Appendix B.

Theoretical error: In order to validate FEA results, stresses were compared to theoretical calculations as well as experimental values (see Appendix B for theoretical calculations). Unfortunately, theoretical calculations were only feasible for hoop stress calculations under internal pressure, so theoretical error calculations for the static loading cases were unavailable. Using theoretical calculations as "truth" values, errors encountered when comparing FEA results to theoretical results were relatively low - 4.53% for LEF2LSO and .83% for LEF5LHDU. These error values do not take into account the results at the lowest pressure level, 500 psi, as it seems that the FEA model overpredicts the stiffness of the Titanium material of the line at such a low pressure, causing high error due to a negative offset. However, above that pressure level, theoretical error levels were consistently low as just mentioned.

Experimental error: Comparing FEA results to experimental results yielded higher error. Using experimental results as "truth" values, average experimental error in the LEF2LSO line was 10.89%, again discounting errors due to the tendency of the FEA model to overpredict line stiffness. Average experimental error for the LEF5LHDU model was high, 79.16%, also discounting the 500 psi anomaly in the FEA model. Stresses in the LEF5LHDU FEA model were consistently much higher than in the calibrations, again with the exception of the 500 psi. One source of error for the LEF5LHDU model is the technique in which force was applied to the experimental calibration. The model was loaded at a point very close to the physical location of the strain gage. The resulting stresses in the FEA model had very high gradients in the vicinity of the load application, causing precise readings of stress in the area where the strain gage was located to be somewhat difficult. Another possible explanation for this large error is a discrepancy in the installation procedure of the strain gage. The gages were to be wired in such a manner as to nullify any stresses due to bending in the line; both lines were wired in this manner. In addition, they were to be oriented at an angle (dependant on the material of the line) relative to the hydraulic line axis in order to compensate for the Poisson effect (the tendency of the line to deform in both the radial and axial directions - pressure should only be measured due to radial, not axial, expansion). The strain gages on the LEF2LSO line were installed at this prescribed angle, but the gages on the LEF5LHDU line were instead aligned with the axis of the hydraulic line. It is possible that the small radius of the LEF5LHDU line precluded installing the gages at an angle to the axis. However, the line will still exhibit Poisson effects. Although this definitely affects the measuring of hoop stress on the line, it is believed that this oversight alone is not enough to explain the high errors encountered. Another contributing factor is the poor temperature compensation exhibited by the LEF5LHDU line. This could be a possible indication of other strain gage installation-related errors, since the lack of temperature compensation is most likely a wiring issue. There are numerous factors involved in the installation of strain gages that can contribute to error; even the most meticulous application typically results in at best approximately 5% error (Measurement Systems), so the observed discrepancies in installation issues can easily explain some of the errors observed in both lines.

CONCLUSIONS

The data clearly shows that strain gages respond to not only hoop stress but also to other external forces on hydraulic lines. The Uncertainty levels for the two gages tested was approximately 20%, compared to approximately 2.5% for pressure transducers – the strain gages displayed nearly a full order of magnitude more measurement uncertainty. It is recommended that strain gages be used only when "approximate" data is required, or for trend data. They should not be used for precise measurement of hydraulic line pressures during flight. Safety of flight may be more at risk if precise knowledge of hydraulic line pressure is required for go/no-go decisions. The FEA model conformed closely to the theoretical calculations of hoop stress due to internal pressure only, but in both lines, higher errors were encountered when comparing to experimental results. The high disparity between FEA results and LEF5LHDU results is especially obvious, but the multiple procedural errors in gage installation at least partially ameliorate these results. The application of torque to the FEA model showed that such a load would contribute to hoop stress in the lines, and therefore cause imprecise readings of pressure in the line. If torque was imposed on the line by preloading it during installation or via a flight load under certain conditions, it could definitely be an error source in the measurement of pressure. Other dynamic, thermal, and static loading conditions could potentially impose loads on the lines, and may warrant further exploration to determine their impact.

APPENDIX A: CALCULATIONS AND NUMERICAL DATA

Calculations for Strain Gage and Pressure transducer uncertainty:

1. **General.** The calibrations were performed under conditions employing 5 independent variables: Parameter (2), Transducer (2), Pressure (5), Force type (5), and Temperature (5). Total number of combinations was 2 x 2 x 5 x 5 x 5 = 500. MS Access was used to select and group appropriate combinations and to perform the calculations. The total number of point pairs was 3,408. The data was equally split between strain gage and pressure transducer calibrations. Approximately 75% of the data was gathered from LEF2LSO, with the remaining 25% from LEF5LHDU.
2. **Truth data**. Select the unstrained data at 70°F. 208 point pairs total
   a.) **Truth-value (mVolts) at each pressure**. Take the average and standard deviation of all point pairs grouped by pressure, transducer type, and parameter name. (20 values)
   b.) **Truth range (mVolts)**. Subtract the zero psig truth-value from the 2000 psig truth-value for each transducer type and parameter name. (4 values)
3. **Bias and Scatter values**. Select all data. 3,408 point pairs total.
   a.) **Diff (mVolts)**. Subtract the appropriate Truth-value from each Output. (3,408 values)
   b.) **Diff (%).** Divide Diff (mVolts) by the truth range, and multiply by 100%. (3,408 values)
   c.) **B (%).** Take the average of Diff (%), grouped by transducer type and parameter name. (4 values)
   d.) **S (%).** Take the standard deviation of Diff (%) grouped by transducer type and parameter name. (4 values)
4. **U_{95} values.** Calculate U_{95} in % using the Abernethy equation below. (4 values)
   Abernethy U_{95} equation:

   $$U_{95} = \pm\sqrt{B^2 + (2S)^2} \qquad \text{(Equation 1)}$$

5. **Force Effects.** Calculate B and S over all data, with additional grouping by force category.
   a) **Truth-value (mVolts) at each pressure.** Use the values calculated in 2a above.
   b) **Truth range (mVolts).** Use the truth range calculated in 2b above.
   c) **Bias and Scatter values.** Select all data. 3,408 point pairs total.
   d) **Diff (mVolts).** Use the values calculated in 3a above.
   e) **Diff (%).** Use the values calculated in 3b above.
   f) **Bforce (%).** Take the average of Diff (%), grouped by transducer type, parameter name, and force category. (20 values)
   g) **Sforce (%).** Take the standard deviation of Diff (%), grouped by transducer type, parameter name, and force category. (20 values)
   h) **U_{95}force (%).** Calculate U_{95}force using the equation in 4 above.
6. **Temperature Effects.** Calculate B and S over all data, with additional grouping by temperature.
   a) **Truth-value (mVolts) at each pressure.** Use the values calculated in 2a above.
   b) **Truth range (mVolts).** Use the truth range calculated in 2b above.
   c) **Bias and Scatter values.** Select all data. 3,408 point pairs total.
   d) **Diff (mVolts).** Use the values calculated in 3a above.
   e) **Diff (%).** Use the values calculated in 3b above.
   f) **Btemp (%).** Take the average of Diff (%), grouped by transducer type, parameter name, and temperature. (20 values)

g) **Stemp (%).** Take the standard deviation of Diff (%), grouped by transducer type, parameter name, and temperature. (20 values)

h) **U_{95}temp (%).** Calculate U_{95}temp using the equation given in 4 above.

7. **Slope, y-intercept, and R2 correlation.** Plot the point pairs in Microsoft Excel and use that application to calculate these parameters.
8. **Results.** The results of the calculations are tabulated on the following pages.

Figure 12: LEF2LSO Truth Data with Line Equations and Correlation

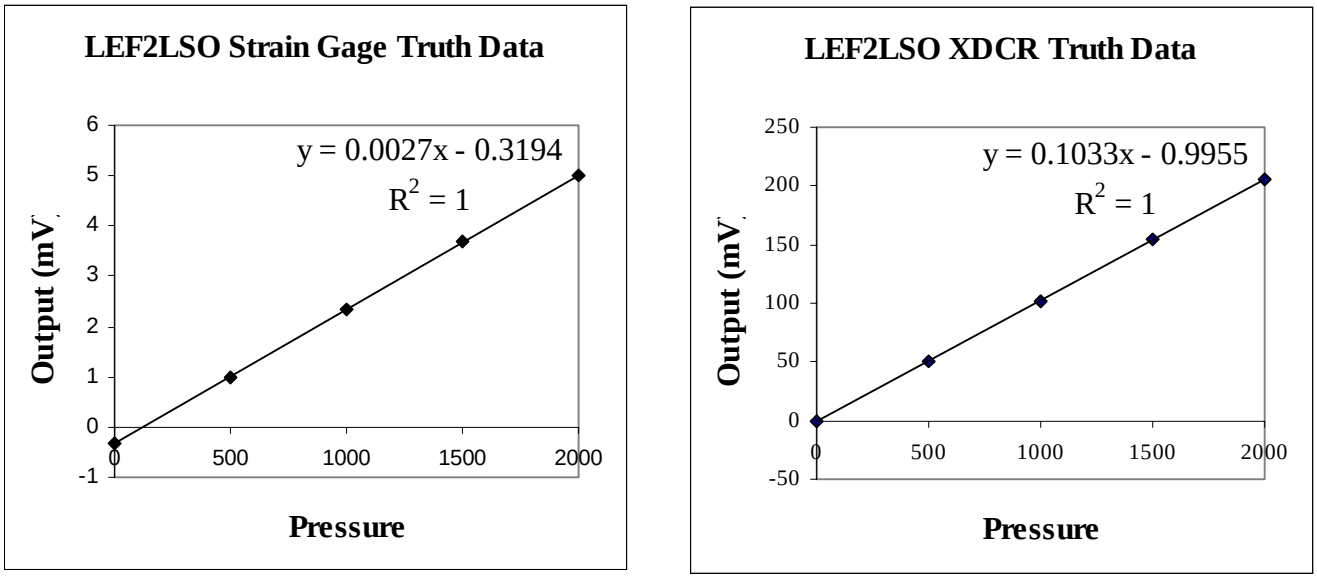

Figure 13: LEF5LHDU Truth Data with Line Equation and Correlations

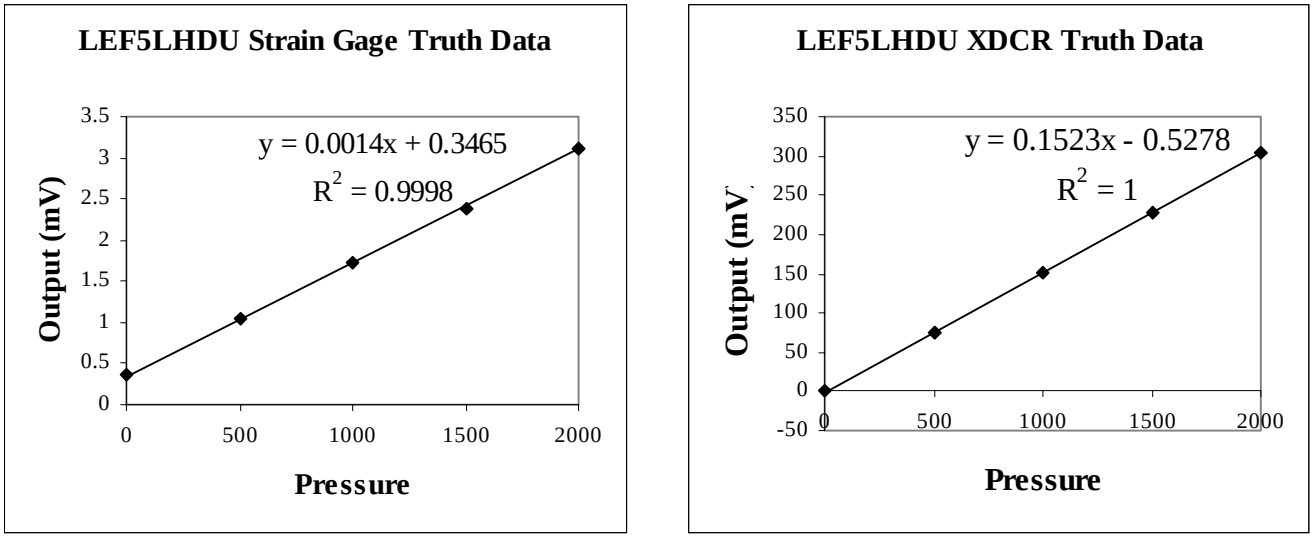

Table 2: Truth data

Parameter	Transducer	Pressure	Truth Range (mV)	Truth Output (mV)
LEF2LSO	Strain Gage	0	5.31547	-0.31983333
LEF2LSO	Strain Gage	500	5.31547	1.007749995
LEF2LSO	Strain Gage	1000	5.31547	2.342666646
LEF2LSO	Strain Gage	1500	5.31547	3.683500032
LEF2LSO	Strain Gage	2000	5.31547	4.99563642
LEF2LSO	XDCR	0	206.6542	-1.163999985
LEF2LSO	XDCR	500	206.6542	50.73333327
LEF2LSO	XDCR	1000	206.6542	102.5379995
LEF2LSO	XDCR	1500	206.6542	154.1354179
LEF2LSO	XDCR	2000	206.6542	205.4902496
LEF5LHDU	Strain Gage	0	2.764196	0.356375001
LEF5LHDU	Strain Gage	500	2.764196	1.034249999
LEF5LHDU	Strain Gage	1000	2.764196	1.715500012
LEF5LHDU	Strain Gage	1500	2.764196	2.393875033
LEF5LHDU	Strain Gage	2000	2.764196	3.120571443
LEF5LHDU	XDCR	0	304.6169	-0.237400006
LEF5LHDU	XDCR	500	304.6169	75.4865509
LEF5LHDU	XDCR	1000	304.6169	151.4796021
LEF5LHDU	XDCR	1500	304.6169	227.7920471
LEF5LHDU	XDCR	2000	304.6169	304.3795013

Table 3: Force Effects – Bias, Scatter, and U_{95}

Parameter	Transducer	ForceCat	BForce	SForce	U95Force
LEF2LSO	Strain Gage	C	18.40%	0.92%	18.49%
		D	-2.49%	0.79%	2.96%
		T	-5.43%	1.12%	5.87%
		Un	-0.93%	2.02%	4.15%
		Up	-6.78%	0.97%	7.05%
	XDCR	C	0.31%	1.07%	2.16%
		D	0.43%	1.08%	2.19%
		T	0.59%	1.18%	2.44%
		Un	-0.47%	1.40%	2.84%
		Up	0.53%	1.32%	2.68%
	Strain Gage	C	-15.97%	5.10%	18.95%
		D	-14.39%	3.37%	15.89%
		T	-5.50%	7.75%	16.44%
		Un	5.90%	8.32%	17.66%

Parameter	Transducer	ForceCat	BForce	SForce	U95Force
LEF5LHDU		Up	-2.75%	3.44%	7.41%
	XDCR	C	0.81%	2.04%	4.17%
		D	-0.07%	0.75%	1.50%
		T	0.23%	0.62%	1.26%
		Un	-0.27%	0.50%	1.04%
		Up	-0.12%	0.73%	1.47%

Table 4: LSBF slope, intercept, and correlation of strain gage LEF2LSO point pairs grouped by force type

	C	Un	D	T	Up	Averages
m =	0.0026918	0.0026856	0.0026744	0.0025937	0.0027099	0.002671
b =	0.628002	-0.393034	-0.465064	-0.540292	-0.7282	-0.29972
R2 =	0.994847	0.9969001	0.9995502	0.9996625	0.9996114	0.999042

Table 5: LSBF slope, intercept, and correlation of pressure transducer LEF2LSO point pairs (ungrouped)

	All
m =	0.103102
b =	-0.20556
R2 =	0.998688

Table 6: LSBF slope, intercept, and correlation of strain gage LEF5LHDU point pairs grouped by force type

	Un	Up	T	D	C	Averages
m =	0.001365	0.001341	0.001336	0.001345	0.001339	0.001345
b =	0.522049	0.3068	0.236086	-0.01893	-0.05601	0.197998
R2 =	0.946383	0.991117	0.952808	0.991374	0.979592	0.972255

Table 7: LSBF slope, intercept, and correlation of pressure transducer LEF5LHDU point pairs (ungrouped)

	All
m =	0.151632
b =	0.254199
R2 =	0.99912

Table 8: Temperature effects – Bias, Scatter, and U_{95}

Parameter	Transducer	Temperature	BTemp	STemp	U95Temp
LEF2LSO	Strain Gage	32	0.00%	9.33%	18.67%
		70	0.74%	9.27%	18.56%
		100	0.66%	9.13%	18.28%
		150	0.97%	9.07%	18.17%
		200	0.27%	9.13%	18.26%
	XDCR	32	1.01%	0.75%	1.81%
		70	0.90%	0.75%	1.75%
		100	1.02%	0.68%	1.71%
		150	-0.06%	0.99%	1.98%
		200	-1.60%	0.74%	2.18%
LEF5LHDU	Strain Gage	32	-5.54%	0.83%	5.79%
		70	-10.40%	9.14%	21.02%
		100	11.35%	0.72%	11.44%
		150	12.31%	0.56%	12.36%
		200	-2.10%	9.22%	18.56%
	XDCR	32	-0.26%	0.41%	0.86%
		70	0.35%	0.27%	0.65%
		100	0.01%	0.24%	0.49%
		150	-0.32%	0.07%	0.35%
		200	-0.26%	1.70%	3.41%

Table 9: LSBF slope, intercept, and correlation of strain gage LEF2LSO point pairs (ungrouped)

	All
m =	0.002671
b =	-0.30124
R2 =	0.937454

Table 10: LSBF slope, intercept, and correlation of strain gage LEF5LHDU point pairs grouped by temperature

	150	100	200	32	70	Averages
m =	0.001368	0.001357	0.001351	0.001352	0.001339	0.001353
b =	0.696233	0.680867	0.315013	0.218467	0.097757	0.401667
R2 =	0.999997	0.999997	0.934479	0.999993	0.93443	0.973779

Table 11:LSBF slope, intercept, and correlation of pressure transducer LEF5LHDU point pairs grouped by temperature

	200	32	70	100	150	Averages
m =	0.15015	0.15058	0.15251	0.15333	0.15254	0.15182
b =	0.84621	0.4123	0.34959	-1.5254	-1.7203	-0.3275
R2 =	0.99786	0.99999	0.99994	0.99999	1	0.99956

Table 12: Overall Bias, Scatter, U_{95}

Parameter	Transducer	B	S	U95
LEF2LSO	Strain Gage	0.53%	9.18%	18.37%
LEF2LSO	XDCR	0.27%	1.28%	2.57%
LEF5LHDU	Strain Gage	-4.05%	11.00%	22.37%
LEF5LHDU	XDCR	0.04%	1.06%	2.11%

APPENDIX B: FEA CALCULATIONS AND NUMERICAL DATA

Theoretical calculations:

Hoop strains and stresses were calculated from the four applied pressures.

$$\varepsilon_H = \frac{PD_i}{E2t}(1-.5\mu)$$

ε_H - hoop strain (in/in)
P - pressure = 500, 1000, 1500, 2000 psi
D_i - inner diameter = .448 in (LEF2LSO), .234 in (LEF5LHDU)
E - Young's modulus = 16×10^6 psi (Ti-3Al-2.5V Titanium)
t - wall thickness = .026 in (LEF2LSO), .016 in (LEF5LHDU)
μ - Poisson ratio = .3 (Ti-3Al-2.5V Titanium)

$$\sigma_H = \frac{PD_i}{2t}$$

σ_H - hoop stress (psi)

Experimental calculations:

Hoop strains and stresses were calculated from output voltages of the strain gages during the calibration runs. Theoretical error was calculated using theoretical calculations as "truth" values.

$$\varepsilon_H = \left(\frac{V_o}{V_{in}}\right)\left(\frac{4}{G}\right)$$

V_o - output voltage (mV)
V_{in} - input voltage = 10 V
G - strain gage factor = 2.07 [Micro Measurements type EK(XX)-210EA-10C(SE) strain gage]

$$\sigma_H = E\varepsilon_H$$

FEA calculations:

Hoop stresses were read from the elements in the FEA model corresponding to the strain gage locations on the hydraulic lines. Theoretical error was calculated using theoretical calculations as "truth" values, and experimental error was calculated using experimental results as "truth" values.

Results:

The FEA results are tabulated in the following pages.

Table 13 – LEF2LSO FEA results

			Theoretical calcs.			Experimental results				ANSYS model			
P (psi)	Load Value	Load Dir.	ε_H	σ_H (psi)	average V_o (mV)	average ε_H	theo. error	average σ_H (psi)	theo. error	Load Case(s)	σ_H (psi)	theo. error	exper. error
static													
2000	0		9.012E-04	17230.77	5.338	1.031E-03	14.46%	16503.65	-4.22%	1	18012	4.53%	9.14%
1500	0		6.759E-04	12923.08	3.994	7.718E-04	14.20%	12349.22	-4.44%	2	13509	4.53%	9.39%
1000	0		4.506E-04	8615.38	2.656	5.133E-04	13.92%	8213.02	-4.67%	3	9005.8	4.53%	9.65%
500	0		2.253E-04	4307.69	1.325	2.559E-04	13.60%	4095.07	-4.94%	4	3375.6	-21.64%	-17.57%
0	0				-0.383	average offset							
"up"													
2000	25	FY			5.384	1.040E-03		16644.64		5+1	18033		8.34%
1500	25	FY			4.027	7.782E-04		12450.63		5+2	13539		8.74%
1000	25	FY			2.678	5.174E-04		8278.26		5+3	9052.3		9.35%
500	25	FY			1.337	2.583E-04		4132.17		5+4	3483		-15.71%
0	25	FY			-0.744	average offset							
"tension"													
2000	25.5	FZ			5.148	9.948E-04		15917.55		6+1	18130		13.90%
1500	25.5	FZ			3.848	7.436E-04		11897.71		6+2	13631		14.57%
1000	25.5	FZ			2.557	4.941E-04		7905.19		6+3	9133.1		15.53%
500	25.5	FZ			1.276	2.465E-04		3944.09		6+4	3736		-5.28%
0	25.5	FZ			-0.489	average offset							
"down"													
2000	-30	FY			5.315	1.027E-03		16432.85		7+1	18056		9.88%
1500	-30	FY			3.973	7.678E-04		12284.19		7+2	13574		10.50%
1000	-30	FY			2.641	5.103E-04		8164.38		7+3	9116.5		11.66%
500	-30	FY			1.316	2.543E-04		4069.31		7+4	3844.1		-5.53%
0	-30	FY			-0.448	average offset							
"compression"													
2000	?	FZ			6.473	1.251E-03		20012.93		8+1	17996		-10.08%
1500	?	FZ			5.119	9.892E-04		15826.65		8+2	13495		-14.73%
1000	?	FZ			4.077	7.878E-04		12604.70		8+3	8994.1		-28.64%
500	?	FZ			2.443	4.721E-04		7553.03		8+4	3372		-55.36%
0	?	FZ			0.671	average offset							
torque CCW													
2000	30	MZ								9+1	18274		
1500	30	MZ								9+2	13860		
1000	30	MZ								9+3	9516.4		
500	30	MZ								9+4	4360.7		
0	30	MZ								9	1660.5		
torque CW													
2000	-30	MZ								10+1	18013		
1500	-30	MZ								10+2	13510		
1000	-30	MZ								10+3	9007		
500	-30	MZ								10+4	3377.1		
0	-30	MZ								10	1629.5		

Table 14 – LEF5LHDU FEA results

				Theoretical calcs.		Experimental results					ANSYS model			
P (psi)	T (°F)	Load Value	Load Dir.	ε_H	σ_H (psi)	average V_o (mV)	average ε_H	theo. error	average σ_H (psi)	theo. error	Load Case(s)	σ_H (psi)	theo. error	exper. error
static														
2000	70	0		7.649E-04	14625.00	2.707	5.232E-04	-31.60%	8370.50	-42.77%	1	14746	0.83%	76.17%
1500	70	0		5.737E-04	10968.75	2.031	3.924E-04	-31.60%	6277.87	-42.77%	2	11060	0.83%	76.17%
1000	70	0		3.824E-04	7312.50	1.355	2.617E-04	-31.56%	4187.83	-42.73%	3	7373	0.83%	76.06%
500	70	0		1.912E-04	3656.25	0.675	1.305E-04	-31.76%	2087.99	-42.89%	4	1833	-49.87%	-12.21%
0	70	0				0.471	average offset							
"up"														
2000	70	19.7	FY			2.655	5.130E-04		8207.92		5+1	14719		79.33%
1500	70	19.7	FY			1.989	3.844E-04		6150.72		5+2	11033		79.38%
1000	70	19.7	FY			1.326	2.563E-04		4100.87		5+3	7346		79.13%
500	70	19.7	FY			0.661	1.277E-04		2042.90		5+4	1832		-10.32%
0	70	19.7	FY			-0.166	average offset							
"down"														
2000	70	-32	FY			2.666	5.151E-04		8241.93		6+1	14699		78.34%
1500	70	-32	FY			1.996	3.857E-04		6170.82		6+2	11013		78.47%
1000	70	-32	FY			1.331	2.573E-04		4116.33		6+3	7326		77.97%
500	70	-32	FY			0.660	1.275E-04		2039.81		6+4	1786.5		-12.42%
0	70	-32	FY			0.055	average offset							
"tension"														
2000	70	-18	FZ			2.678	5.174E-04		8278.26		7+1	14741		78.07%
1500	70	-18	FZ			2.004	3.871E-04		6194.40		7+2	11055		78.47%
1000	70	-18	FZ			1.338	2.585E-04		4135.78		7+3	7368		78.15%
500	70	-18	FZ			0.668	1.290E-04		2064.80		7+4	1834.5		-11.15%
0	70	-18	FZ			-0.088	average offset							
"compression"														
2000	70	16.5	FZ			2.667	5.153E-04		8245.28		8+1	14723		78.56%
1500	70	16.5	FZ			1.833	3.542E-04		5666.73		8+2	11037		94.77%
1000	70	16.5	FZ			1.333	2.576E-04		4122.38		8+3	7350.4		78.30%
500	70	16.5	FZ			0.667	1.289E-04		2061.71		8+4	1810.6		-12.18%
0	70	16.5	FZ			0.400	average offset							

ACKNOWLEDGEMENTS

Jim Farrell, Dwaine Fowler, Doug Mullins, Curt Foianini, Tony Cullison, Gary Rumsey, Ted Delbo

REFERENCES

Dieck, Ronald, Measurement Uncertainty Methods and Applications, Second Edition, Instrument Society of America, Research Triangle Park, NC, 1997.

Abernethy, R.B., and Thompson, Jr., J.W., "Measurement Uncertainty Handbook," Report # AEDC-TR-73-5 / ARO-ETF-TR-72-60, Arnold Engineering Development Center, Arnold Air Force Station, Tennessee, February 1973, Revised January 1980.

Beer, Ferdinand P. and Johnston, E. Russell, Mechanics of Materials, McGraw-Hill Book Company, New York, 1981.

Eagleton, R.H., "Flight Test Aircraft Standard Strain Gage Installation Procedures and Practices Rev D," MDC A0499, McDonnell Douglas Aerospace-East, St. Louis, MO, September 1994.

Measurements Group, Inc., Strain Measuring Systems SC-300 Class Notes, Measurements Group, Inc., Raleigh, NC, 1997.

Young, Warren C., Roark's Formulas for Stress & Strain, Sixth Edition, McGraw-Hill Book Company, New York, 1989.